

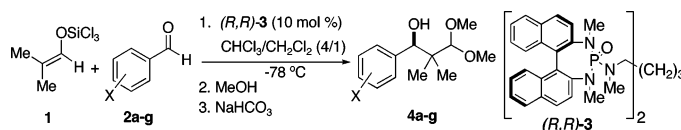
## Mechanistic Insights into the Chiral Phosphoramidate-Catalyzed, Enantioselective Crossed-Aldol Reactions of Aldehydes

Scott E. Denmark\* and Tommy Bui

Department of Chemistry, Roger Adams Laboratory, University of Illinois, Urbana, Illinois 61801

denmark@scs.uiuc.edu

Received August 9, 2005



The mechanism of the phosphoramidate-catalyzed enantioselective aldol additions of trichlorosilyl enolate **1** to aldehydes has been studied. Natural abundance  $^{12}\text{C}/^{13}\text{C}$  kinetic isotope analysis showed that the rate-determining step of the reaction is the aldolization. Arrhenius activation parameters for the aldol addition reaction were determined. The entropy of activation is large and highly negative, whereas the enthalpy of activation is relatively small. Despite the different trends in selectivity observed for electron-rich and electron-poor aldehydes, similar entropic and enthalpic contributions to the free energies of activation are found for both classes of substrates. The experimental results from the Arrhenius and the kinetic isotope effect studies allowed the formulation of an interpretation for the divergent selectivity trends in the aldol reaction.

### Introduction

Recent disclosures from these laboratories have shown that Lewis base catalyzed enantioselective aldol reactions are a synthetically viable method for the construction of oxygenated carbon chains in a stereoselective fashion.<sup>1</sup> A significant portion of these findings arises from the results of previous studies on the Lewis base catalyzed aldol addition of trichlorosilyl enolates to various aldehydes.<sup>2</sup> These earlier studies showed that in the presence of a catalytic amount of a chiral Lewis base, trichlorosilyl enolates derived from both esters<sup>3</sup> and ketones<sup>4</sup> react smoothly with aldehydes to afford aldol products in high yield with good to excellent enantio- and diastereoselectivity. A unique feature of this type of aldol reaction is

the dependence of diastereoselectivity on enolate geometry, thus allowing access to both the syn and anti aldol product architectures by the use of *Z*- and *E*-trichlorosilyl enolates, respectively.

In recent years, the Lewis base catalyzed aldol addition of aldehyde-derived trichlorosilyl enolates to a wide range of aldehydes has also been achieved.<sup>5,6</sup> This directed, crossed-aldol addition affords products in excellent yield and diastereoselectivity albeit moderate to good enantioselectivity. Like the aldol reaction of trichlorosilyl enolates derived from ketones, the diastereoselectivity in the crossed-aldol reaction of aldehydes is also dependent on enolate geometry, indicating that a similar mechanism may be operative for both classes of enolates.

The mechanism of this aldolization process is likely consistent for all classes of trichlorosilyl enolate structures. Specifically, the chiral Lewis base (LB) is believed to bind to the silicon atom of the trichlorosilyl enolate, resulting in ionization of chloride and generation of a cationic silicon species (**i**) (Scheme 1).<sup>7,8</sup> This cationic silicon species binds to the carbonyl oxygen of the

(1) (a) Denmark, S. E.; Wynn, T.; Beutner, G. L. *J. Am. Chem. Soc.* **2002**, *124*, 13405–13407. (b) Denmark, S. E.; Beutner, G. L. *J. Am. Chem. Soc.* **2003**, *125*, 7800–7801. (c) Denmark, S. E.; Fujimori, S. *J. Am. Chem. Soc.* **2005**, *127*, 8971–8973. (d) Denmark, S. E.; Beutner, G. L.; Wynn, T.; Eastgate, M. D. *J. Am. Chem. Soc.* **2005**, *127*, 3774–3789. (d) Denmark, S. E.; Fujimori, S. In *Modern Aldol Reactions*; Mahrwald, R. Ed.; Wiley-VCH: Weinheim, 2004; Vol. 2, Chapter 7. (2) (a) Denmark, S. E.; Stavenger, R. A. *Acc. Chem. Res.* **2000**, *33*, 432–440. (b) Denmark, S. E.; Stavenger, R. A.; Su, X.; Wong, K.-T. *J. Am. Chem. Soc.* **1999**, *121*, 4982–4991.

(3) (a) The enhanced reactivity of trichlorosilyl enolates derived from esters allows them to react with aldehydes even in the absence of Lewis bases: Denmark, S. E.; Winter, S. B. D.; Su, X.; Wong, K.-T. *J. Am. Chem. Soc.* **1996**, *118*, 7404–7405. (b) Lewis base catalyzed enantioselective aldol addition of trichlorosilyl ketene acetal to ketones: Denmark, S. E.; Fan, Y. *J. Am. Chem. Soc.* **2002**, *124*, 4233–4235.

(4) (a) Denmark, S. E.; Stavenger, R. A.; Su, X.; Wong, K.-T.; Nishigaishi, Y. *Pure Appl. Chem.* **1998**, *70*, 1469–1476. (b) Denmark, S. E.; Stavenger, R. S.; Wong, K.-T. *J. Org. Chem.* **1998**, *63*, 918–919.

(5) Denmark, S. E.; Ghosh, S. K. *Angew. Chem., Int. Ed.* **2001**, *40*, 4759–4762.

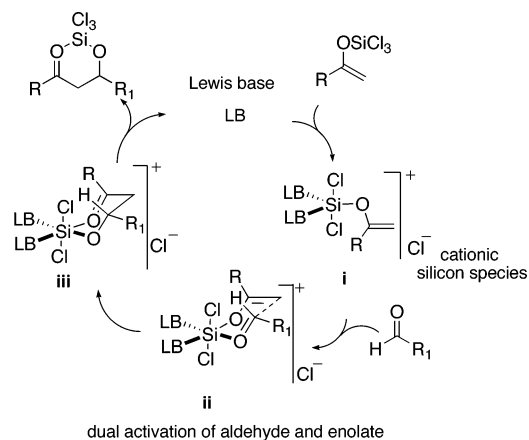
(6) Denmark, S. E.; Bui, T. *Proc. Nat. Acad. Sci. U.S.A.* **2004**, *101*, 5439–5444.

(7) Mechanistic studies of Lewis base catalyzed aldol reactions: (a) Denmark, S. E.; Pham, S. M. *Helv. Chim. Acta* **2000**, *83*, 1846–1853. (b) Denmark, S. E.; Su, X. *Tetrahedron* **1999**, *55*, 8727–8738. (c) Denmark, S. E.; Barsanti, P. A. *J. Org. Chem.* **1998**, *63*, 2428–2429.

(8) Berrisford, D. J.; Short, J. D.; Attenoux, S. *Tetrahedron Lett.* **1997**, *38*, 2351–2354.

aldehyde, generating a ternary complex (ii) that undergoes reaction through a closed six-membered transition state structure. The cationic silicon atom thus acts as an organizational center, binding and activating both the electrophile and the nucleophile. Common ion effect studies support the hypothesis that prior ionization of chloride from the trichlorosilyl enolate occurs upon binding of the Lewis base.<sup>9</sup> In addition, both kinetic and nonlinear effect studies have revealed that two mechanistic pathways for the aldol reactions can be operative depending on the structure of the catalyst.<sup>7a,9</sup>

## SCHEME 1



In the course of examining the scope of the crossed-aldol reaction of aldehydes, we were surprised to find that there is a linear but divergent dependence of enantiomeric ratio on the electronic nature of aldehyde substituent.<sup>6,10</sup> To better understand the origin and significance of this phenomenon, studies on the mechanism of the Lewis base-catalyzed, crossed-aldol reactions of aldehydes have been undertaken. Of particular interest was to establish the rate- and stereochemistry-determining steps of this aldol reaction. Two limiting scenarios for these steps were considered: (1) the binding of the aldehyde to the silicon atom or (2) the aldolization.<sup>11</sup> To probe this question, <sup>12</sup>C/<sup>13</sup>C kinetic isotope effects at natural abundance as pioneered by Singleton was employed to determine whether the binding of aldehyde to the silicon atom or the aldolization is the rate-determining step.<sup>12</sup> An alternative interpretation of the divergent selectivity observed for electron-rich and electron-poor aldehydes was proposed to involve a change in the dominance of entropic or enthalpic contributions to the free energies of activation for the two competing diastereomeric transition structures.<sup>13</sup> For this reason, Arrhenius studies<sup>14</sup> were also conducted to examine the

(9) Denmark, S. E.; Su, X.; Nishigaishi, Y. *J. Am. Chem. Soc.* **1998**, *120*, 12990–12991.

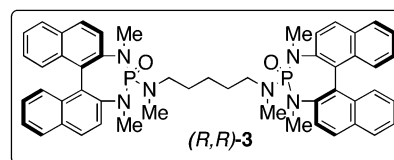
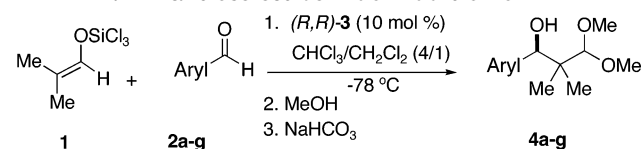
(10) A modest trend in enantio- and diastereoselectivity due to substituent effects was observed previously: Denmark, S. E.; Stavenger, R. A.; Wong, K.-T. *Tetrahedron* **1998**, *54*, 10389–10492.

(11) Ionization of chloride from the trichlorosilyl enolate is reversible and thus unlikely to be the rate-determining step. See ref 9.

(12) (a) Singleton, D. A.; Thomas, A. A. *J. Am. Chem. Soc.* **1995**, *117*, 9357–9358. (b) Singleton, D. A.; Snyder, J. P.; Frantz, D. E. *J. Am. Chem. Soc.* **1997**, *119*, 3383–3384. (c) Singleton, D. A.; DelMonte, A. J.; Meyer, M.; *J. Am. Chem. Soc.* **1999**, *121*, 10865–1074.

(13) (a) Cainelli, G.; Giacomini, D.; Galletti, P. *Eur. J. Org. Chem.* **1999**, *1*, 61–65. (b) Sugimura, T.; Tei, T.; Mori, A.; Okuyama, T.; Tai, A. *J. Am. Chem. Soc.* **2000**, *122*, 2128–2129.

TABLE 1. Enantioselective Aldol Addition of 1



entry	aryl	product	time, h	yield, % <sup>a</sup>	er <sup>b</sup>
1	C <sub>6</sub> H <sub>5</sub>	<b>4a</b>	8	86	70.0/30.0
2	4-MeC <sub>6</sub> H <sub>4</sub>	<b>4b</b>	12	90	73.0/27.0
3	4-MeOC <sub>6</sub> H <sub>4</sub>	<b>4c</b>	20	92	75.5/24.5
4	3,4,5-(MeO) <sub>3</sub> C <sub>6</sub> H <sub>2</sub>	<b>4d</b>	26	80	87.5/12.5
5	4-ClC <sub>6</sub> H <sub>4</sub>	<b>4e</b>	8	85	89.0/11.0
6	4-CF <sub>3</sub> C <sub>6</sub> H <sub>4</sub>	<b>4f</b>	8	86	90.0/10.0
7	4-NO <sub>2</sub> C <sub>6</sub> H <sub>4</sub>	<b>4g</b>	8	89	91.0/9.0

<sup>a</sup> Yield of analytically pure materials. <sup>b</sup> er determined by CSP-SFC, Daicel Chiralpak, OD, AS, and AD columns.

activation parameters for the aldol additions, and the results of these studies together with a unified picture of the role of the individual steps in the aldol addition reaction are reported herein.

## Results

**1. Hammett Study.**<sup>15</sup> The aldol addition of enolate **1** (trichlorosilyl enolate of isobutyraldehyde) to a wide range of aldehydes (**2a–g**) with electronically distinct character was examined in the presence of 10 mol % of the dimeric phosphoramidate **3** (Table 1). Moderate to good selectivity was observed for both electron-rich and electron-poor aldehydes. Generally, electron-poor aldehydes required shorter reaction times and underwent aldolization at a rate faster than those observed for electron-rich aldehydes (entries 2–4 vs 5–7).<sup>16</sup> These results implied that aldolization is the rate-determining step, a conclusion later substantiated by the results of natural abundance kinetic isotope effect experiments. Notably, two distinct trends in selectivity appeared when the Hammett plot of the logarithm of enantiomeric ratio versus sigma ( $\sigma$ ) and inductive sigma ( $\sigma_i$ ) values was constructed (Figure 1).<sup>6,17,18</sup> Using benzaldehyde as a reference point, the selectivity increased as aldehydes became either more electron rich or more electron poor (Table 1, entries 1–4 and 5–7). A break in the Hammett plot was also noted,

(14) Schaleger, L. L.; Long, F. A. *Adv. Phys. Org. Chem.* **1963**, *1*, 1–33.

(15) (a) Hammett, L. P. *J. Am. Chem. Soc.* **1937**, *59*, 96–103. (b) Hammett, L. P. *Chem. Rev.* **1935**, *17*, 125–136.

(16) These results are consistent with those obtained from subsequent kinetic studies

(17) If  $\sigma_i$  was not used for the electron-poor aldehyde series, the 4-chloro substituent would be the only scattered data point. The chloro substituent is known to possess both inductive and resonance effects, which are opposed to one another, depending on the nature of the reaction. See: Carey, F. A.; Sundberg, R. J. In *Advanced Organic Chemistry Part A: Structure and Mechanism*; Plenum: New York, 2000; pp 187–226. Substituent effects on enantiomeric ratio: Togni, A.; Pastor, S. S. *J. Org. Chem.* **1990**, *55*, 1649–1664. Bowl-shaped Hammett plot: (a) Bergman, R. G.; Simpson, R. D. *Organometallics* **1993**, *12*, 781–796. (b) Bergman, R. G.; Fulton, J. R.; Holland, A. W.; Fox, D. J. *Acc. Chem. Res.* **2002**, *35*, 44–56.

and it is indicative of either a change in the stereochemistry-determining step or a change in factors that control the selectivity for both classes of aldehydes.<sup>19</sup> Moreover, similar  $\rho$  values of opposite sign were obtained for electron-rich and electron-poor aldehydes, indicating that the sensitivity of the aldol reaction to the electronic effects in both cases occurs at more or less the same extent. The possibility that the products were formed in opposite enantiomeric series was unambiguously ruled out by single crystal, X-ray analysis of the products from **4d** and **4f**.<sup>6</sup>

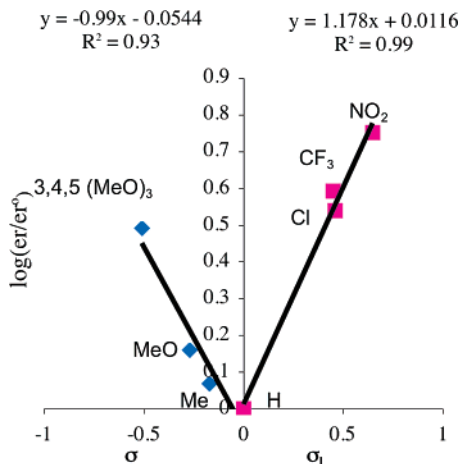


**FIGURE 1.** Substituent effects on enantiomeric ratio in aldol addition of **1** to aromatic aldehydes.

**2. Natural Abundance <sup>12</sup>C/<sup>13</sup>C Isotope Effects.** Aldehydes **2d** and **2f** were chosen as representative substrates for the mechanistic studies and were used in separate, independent kinetic isotope effect experiments (Scheme 2). These aldehydes were chosen to represent the two selectivity regimes seen in the Hammett plot. If aldolization is rate-determining, then significant, positive <sup>12</sup>C/<sup>13</sup>C KIEs will be expected at the α-carbon of the enolate (or an aldehyde carbonyl carbon).<sup>20</sup> On the other hand, if binding is rate-determining, there will be no kinetic isotope effect at either of the reacting carbon atoms. Experimentally, the aldol reactions were run under the standard conditions, except that the enolate was used in excess relative to the aldehyde. The <sup>12</sup>C/<sup>13</sup>C KIEs at the α-carbon of the enolate can be determined by analysis of either residual starting enolate or the aldol product. We chose product analysis and thus used the enolate in large excess.<sup>21</sup> Upon complete consumption of

(18) Hammett substituent constants: (a) Lowry, T. H.; Richardson, K. S. In *Mechanism and Theory in Organic Chemistry*, 2nd ed.; Harper & Row: New York, 1981; p 154. (b) Hansch, C.; Leo, A.; Taft, R. W. *Chem. Rev.* **1991**, *91*, 165–195. (c) Brown, H. C.; McDaniel, D. H. *J. Org. Chem.* **1958**, *23*, 420–427.

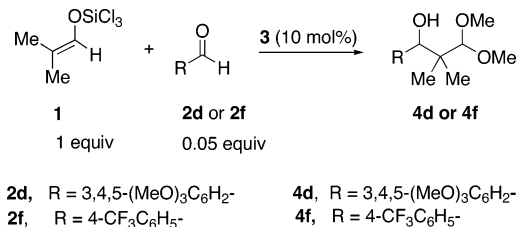
(19) (a) Review on the effects of thermodynamic parameters such as enthalpy and entropy on selectivity: Scharf, H.-D.; Buschmann, H.; Hoffmann, N.; Esser, P. *Angew. Chem., Int. Ed. Engl.* **1991**, *30*, 477–515. (b) Comprehensive review on linear free energy relationships: Leffler, J. E.; Grunwald, E. In *Rates and Equilibria of Organic Reactions*; John Wiley & Sons: New York, 1963; Chapters 6 and 7. (c) Substituent effects on reaction mechanisms: Tsuno, Y.; Fujio, M. *Adv. Phys. Org. Chem.* **1999**, *32*, 267–385.

(20) Melander, L.; Saunders, W. H., Jr. In *Reaction Rates of Isotopic Molecules*; Wiley: New York, 1980; pp 95–102.

(21) By this approach, the isotope effect is manifested in the more rapid uptake of C-12 from the enolate resulting in a depletion of the NMR-active C-13 nucleus at this carbon.

the aldehyde, the reactions were quenched with methanol at  $-78$  °C and subsequently worked up with sodium bicarbonate. The resulting aldol adducts **4d** and **4f** were isolated, purified, and used in the <sup>12</sup>C/<sup>13</sup>C KIE analysis. As reference standards, aldol adducts were also obtained under similar reaction conditions, except using aldehyde and the enolate in a 1:1 ratio.

## SCHEME 2



To obtain accurate integration of the <sup>13</sup>C signals of the aldol adducts, both the relaxation time ( $T_1$ ) and the 90° pulse width were calibrated for each sample. The delay time  $d_1$  was set equal to  $8T_1$  to ensure that all of the carbons were fully relaxed between pulses. The experiments used to obtain the <sup>13</sup>C integrations were performed on a Unity 500 MHz NMR instrument. A sufficient number of scans was taken to ensure that the signal-to-noise ratio was greater than to 250:1. The integrations for the signals of interest were determined by the half-height of the line width of the integrating peak multiplied by 10 on each side. The spectrum of each sample was integrated five times, and the average integration for each carbon signal was then used for <sup>12</sup>C/<sup>13</sup>C KIE analysis. Using C(1'') or C(2'') of the aldol products as an internal standard, substantial <sup>12</sup>C/<sup>13</sup>C KIEs were observed at C(2), the α-carbon of the enolate, suggesting that aldolization is the rate-determining step (Figure 2). This agrees with earlier studies of <sup>12</sup>C/<sup>13</sup>C KIEs in the Lewis base-catalyzed aldol reaction of ketone-derived trichlorosilyl enolates wherein the aldolization step was shown to be the rate-determining step.<sup>22</sup> Similar results were obtained from both electron-rich (**2d**) and electron-poor (**2f**) substrates, indicating that there is no change in the rate-determining step upon changing the electronic nature of aldehydes.

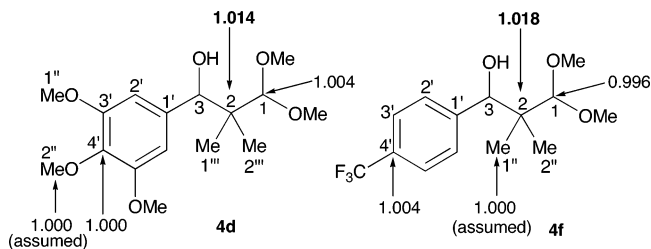


**FIGURE 2.** <sup>12</sup>C/<sup>13</sup>C kinetic isotope effects at C(2).

**2. Arrhenius Activation Parameters.** Because aldolization is the rate-determining step regardless of the electronic character of aldehydes, the enthalpic and entropic contributions to the activation free energy were determined to establish if either was responsible for the divergent selectivity profiles for electron-rich and electron-

(22) Pham, S. Ph.D. Thesis, University of Illinois, Urbana–Champaign, 2002.



poor aldehydes. The Arrhenius parameters for the aldol reaction were determined by measuring the rate constant as a function of temperature. For consistency, aldehydes **2d** and **2f** were chosen for these studies. The aldol reactions were run under the standard conditions, and the reaction temperatures for all the runs were monitored internally.<sup>6</sup> The disappearance of the aldehyde over time was followed by directly monitoring the reaction with ReactIR.<sup>23</sup> Each individual rate constant was then determined from the best-fit line of the plot of time vs  $1/[\text{aldehyde}]$  and exhibited overall second-order dependence for both substrates, indicating that a similar mechanism may be operative for both classes of aldehydes.<sup>24</sup> The rate constant obtained at a given temperature was averaged over two runs (Table 2 and the Supporting Information). From these average rate constants, the graphs of  $k_{\text{obs}}$  vs  $1/T$  for aldehydes **2d** and **2f** were generated (Figures 3 and 4). Arrhenius activation energy parameters could be calculated, and the results are summarized in Table 2.<sup>25</sup>

The Arrhenius studies revealed that, in both cases, the entropy of activation is large and negative, suggesting a highly ordered transition structure for aldolization and that the entropy of activation for aldehyde **2d** is more negative than that of aldehyde **2f**.<sup>26</sup> In contrast, the enthalpy of activation observed in both cases is relatively small. These results are in agreement with those obtained previously for the aldol reactions of ketone-derived trichlorosilyl enolates.<sup>7a</sup> The Arrhenius studies also showed that the free energy of activation for the reaction of aldehyde **2f** is 1.4 kcal/mol less than that of aldehyde **2d**. Experimentally, the rate of aldolization for aldehyde **2f** is faster than that of aldehyde **2d**, and the rate constant for the reaction of **2f** is at least 50-fold greater than the rate constant for **2d** at  $-45\text{ }^{\circ}\text{C}$  (see the Supporting Information).<sup>27</sup> The manifestation of the reactivity of these aldehydes in the rates of aldolization is consistent with the conclusion that aldolization is the rate-determining step. In addition, for both of these electronically distinct aldehydes, the entropy of activation is the major contributor to the free Gibbs energy of activation. The similarities between the kinetic parameters for electron-rich and electron-poor aldehydes hint at a common mechanistic pathway, despite the electronic differences of these substrates.

A notable difference in the preexponential factors for the aldol reactions of aldehydes **2d** and **2f** was observed. The  $A$  value for the reaction of **2d** is small, whereas this value for that of **2f** is exceedingly large (Table 2). It is also noted from Table 2 that there exists an inverse relationship between the preexponential factor  $A$  and the

(23) ReactIR 1000 fitted with a 5/8 in. DiComp Probe, running software Version 2.1a. ASI Applied Systems, Inc., 8223 Cloverleaf Drive, Suite 120, Millersville, MD 21108.

(24) For the graph of time vs  $1/[\text{aldehyde}]$ , see the Supporting Information.

(25) Error analysis for each activation parameters was done according to the previously reported method. Hammett, L. P.; Crowell, T. *J. Am. Chem. Soc.* **1948**, *70*, 3444–3450.

(26) The greater negative activation entropy for **2d** compared to **2f** may arise from the need to freeze out additional degrees of freedom in the methoxy groups to achieve a rigid, ordered transition state in accordance with the Price–Hammett principle. See: Price, F. P., Jr.; Hammett, L. P. *J. Am. Chem. Soc.* **1941**, *63*, 2387–2393.

(27) Even though the aldol reaction of **2b** was run at one-half the concentration of that of **2a**, the  $k_{\text{obs}}$  for **2b** was still about 50-fold greater than that for **2a** at the same temperature.

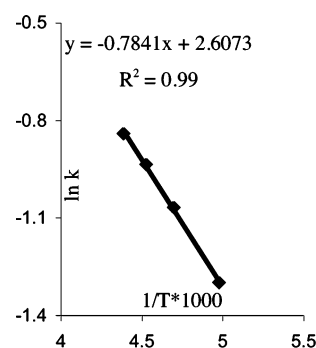


FIGURE 3. Arrhenius plot for **2d**.

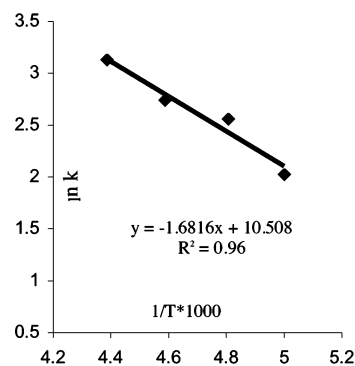


FIGURE 4. Arrhenius plot for **2f**.

entropy of activation. Such an inverse relationship has been pointed out previously.<sup>28</sup>

## Discussion

The foregoing mechanistic experiments allow the identity of the rate- and stereochemistry-determining steps as well as factors that influence selectivity to be addressed. The mechanistic model employed is common to the aldol reactions of ketone-derived trichlorosilyl enolates and therefore involves the intermediacy of an ionized siliconium ion.<sup>8</sup> The initial step, which involves the binding of the Lewis base to the trichlorosilyl enolate, is most likely reversible and has been supported through common ion effect studies.<sup>9</sup> Once this reactive silyl cation is generated, two fundamental steps precede product formation: the binding of the aldehyde to the cationic silicon species and carbon–carbon bond formation (Scheme 3).<sup>7</sup> The working model is supported by previous kinetic studies<sup>7a</sup> wherein the aldol addition reaction exhibits second-order dependence on the phosphoramidate catalysts, which indicates the existence of a siliconium species that can accommodate all of the ligands. The superiority of the dimeric phosphoramidate (*R,R*)-**3** in the crossed-aldol reactions of aldehydes provides support for the premise of the silyl cation intermediate as well.

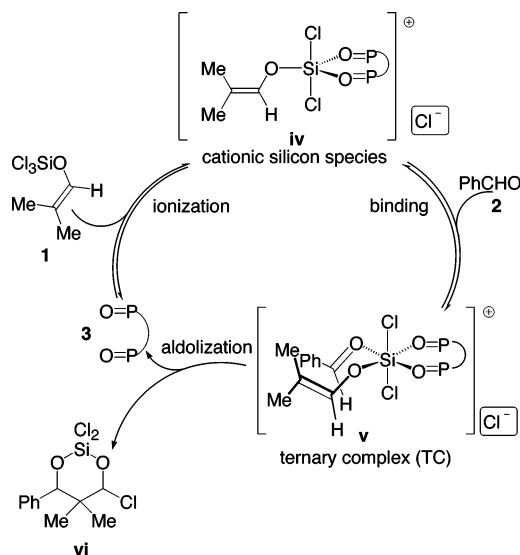
However, ionization of chloride cannot be the rate-determining step and is less likely to be the stereochemistry-determining step due to its reversibility; therefore, the binding of aldehyde or aldolization must serve this role. Four limiting mechanistic scenarios are possible for the pairwise combinations of the rate- and stereochem-

(28) Atkins, P. *Physical Chemistry*; Oxford University Press: New York, 1994; Chapters 25 and 27.

TABLE 2. Arrhenius Activation Energies for Aldol Additions of **2d** and **2f**

RCHO	$k$ , $M^{-1} \text{ min}^{-1}$ ( $-45^\circ \text{C}$ )	$E_a$ , kcal/mol	$A$ , $M^{-1} \text{ S}^{-1}$	$\Delta H^\ddagger$ , kcal/mol	$\Delta S^\ddagger$ , eu	$\Delta G^\ddagger$ , kcal/mol
<b>2d</b>	0.4322	$1.6 \pm 0.1$	$13.4 \pm 0.1$	$1.2 \pm 0.1$	$-54.6 \pm 3$	$12.1 \pm 0.6$
<b>2f</b>	22.57	$3.3 \pm 0.2$	$33900 \pm 1600$	$2.9 \pm 0.1$	$-39.0 \pm 2$	$10.7 \pm 0.5$

SCHEME 3



istry-determining steps (Table 3). Scenario 1 involves a rate-determining binding event, which is followed by a stereochemistry-determining aldolization. Scenario 2 assumes that binding is the both rate- and stereochemistry-determining steps. In scenario 3, a stereochemistry-determining binding event precedes the rate-determining aldolization step. Finally, in scenario 4, aldolization is both the rate- and the stereochemistry-determining steps.

TABLE 3

scenario	rate-determining step	stereochemistry-determining step
1	binding	aldolization
2	binding	binding
3	aldolization	binding
4	aldolization	aldolization

According to the results of  $^{12}\text{C}/^{13}\text{C}$  kinetic isotope studies, the rate-determining step is aldolization regardless of the electronic nature of the substrates, which rules out scenarios 1 and 2. The two remaining scenarios 3 and 4 are difficult to distinguish on the basis of KIE results.

The divergent selectivity observed for electron-rich and electron-poor aldehydes was first postulated to involve a change in the individual entropic and enthalpic contributions to the free energies of activation. However, the Arrhenius studies disproved this hypothesis since in both cases, highly negative and large entropies of activation were observed. Even though the overall pattern of entropic and enthalpic contribution to the free energies of activation is similar, the entropy of activation for the aldol reaction of the electron-rich aldehyde (**2d**) is more negative than that for the aldol reaction of the electron-poor aldehyde (**2f**). This difference in entropy may be due to the added degrees of freedom contributed by the three methoxy groups. According to the Price–Hammett prin-

ciple,<sup>26</sup> the loss of the internal freedom of these methoxy groups on the way to the organized polar transition state for aldolization could account for a greater decrease in entropy.

Despite the break in the Hammett plot of selectivity, these mechanistic studies have led to the conclusion that there is no significant change in mechanism upon changing the electronic nature of aldehyde. No major difference could be found with respect to the kinetic and activation parameters. Moreover, the initial hypothesis for the divergent selectivity that involved a change in the facial orientation of the aldehyde with respect to the enolate was also disproved as both electron-rich and electron-poor substrates gave aldol products with same configuration.<sup>6</sup>

With these possibilities eliminated, we postulated that the divergence in the Hammett plot might involve a change in factors that influence selectivity. To identify these factors, one needs to carefully examine the reactivity and the Lewis basicity of aldehydes and see how the electronic character can influence the two fundamental steps in the proposed mechanism: binding and aldolization. In other words, what are the stereochemical consequences if the aldehyde binds rapidly to the silicon atom and then reacts slowly, or the reverse situation where the aldehyde binds slowly and carbon–carbon bond formation proceeds rapidly. The change in selectivity represents a change in the stereochemistry-determining event without a change in the rate-determining step, i.e., scenarios 3 and 4 are operative for different aldehydes. Alternatively, scenario 4 is operative for both classes of aldehydes, but different factors influence the stereochemical course of the reaction.

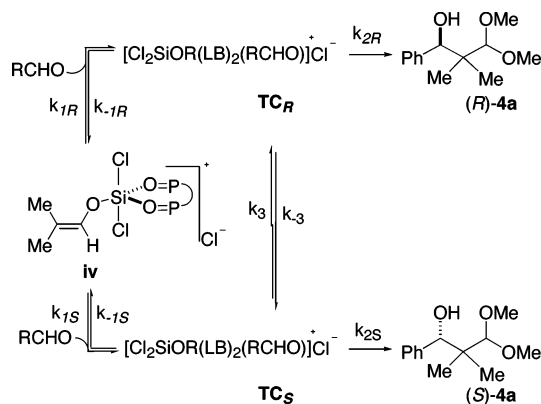
For electron-rich aldehydes, the increased electron density on the carbonyl group renders them more Lewis basic at the oxygen and much less reactive at the carbon than electron-poor substrates. Because of the enhanced Lewis basicity of these aldehydes, they are expected to bind rapidly and favorably to the highly oxophilic, cationic silicon center. The transition state for this binding event is expected to be relatively early. As a result, there is little steric bias present in the formation of the diastereomeric ternary complexes leading to aldol enantiomers. Hence, selectivity mainly arises from the relatively late transition state for aldolization due to the attenuated reactivity of electron rich aldehydes. As the transition state becomes later, the steric interactions between the catalyst/aldehyde complex and the nucleophile are more pronounced. In other words, the later the transition state, the more restrictive it is, leading to more negative entropy of activation (Table 2). In addition, the attenuated reactivity of the electron-rich carbonyl group requires the aldehyde and the enolate to adopt well-defined orientations within the coordination sphere of the silicon center before they can react. This factor and the restriction imposed upon the late transition state for aldolization could account for the smaller value of the

preexponential factor  $A$ , which is a measure of successful collisions (Table 2).

Thus, the rate- and stereochemistry-determining steps both take place during aldolization (scenario 4). According to this analysis, the more electron rich the aldehyde, the later the transition state for aldolization, and the better the selectivity. This trend corresponds to the trend in selectivity seen from the left portion of the Hammett plot.

Alternatively, one can consider that the association of the aldehyde with the cationic silicon species **iv** forms the two ternary complexes,  $\text{TC}_R$  and  $\text{TC}_S$ , leading to the  $R$  and  $S$  aldol enantiomers respectively (Scheme 4). The rates of formation and breakdown between these ternary complexes are designated as  $k_{1R}$  and  $k_{-1R}$  or  $k_{1S}$  and  $k_{-1S}$ , and the rates of aldolization for the  $R$  and the  $S$  aldol enantiomers are  $k_{2R}$  and  $k_{2S}$ , respectively.<sup>29</sup> Because of the attenuated reactivity of electron-rich aldehydes, the energy barrier for aldolization is relatively large for these substrates. This suggests that the rate of interconversion between  $\text{TC}_R$  and  $\text{TC}_S$  must be fast relative to that of aldolization ( $k_{1R}, k_{-1R}, k_{1S}, k_{-1S} \gg k_{2R}, k_{2S}$ ). Under these conditions, the aldol enantiomer product distribution is strictly under Curtin-Hammett control,<sup>30</sup> and enantioselectivities are determined by the difference in the free energies of activation for aldolization,  $\Delta\Delta G^\ddagger$  (Figure 5).

#### SCHEME 4



With electron-poor aldehydes, the decreased electron density at the aldehyde oxygen atoms renders them less Lewis basic and more reactive than electron-rich substrates. This electronic character also manifests itself in the binding and aldolization events. With the attenuated Lewis basicity, the aldehyde binds more slowly and less favorably to the silicon atom, and the energy barrier for this binding tends to be higher as the aldehyde carbonyl becomes less Lewis basic. The transition state for this step is expected to be relatively late in contrast to those for the electron-rich aldehydes.<sup>31</sup> For these reasons, more pronounced steric differentiation between the ternary complexes may occur at a significant degree during the binding event. To achieve selectivity, the transient stereochemical information garnered during this step must

(29) Direct interconversion between  $\text{TC}_R$  and  $\text{TC}_S$  cannot be excluded. For simplicity, it is assumed that  $\text{TC}_R$  and  $\text{TC}_S$  give the  $R$  aldol enantiomer and the  $S$  aldol enantiomer, respectively.

(30) Seeman, J. I. *Chem. Rev.* **1983**, *83*, 83–134.

(31) For electron-poor aldehydes, the energy of the ternary complexes is significantly different from that of the starting aldehyde but similar to that of the transition state structure for aldolization.

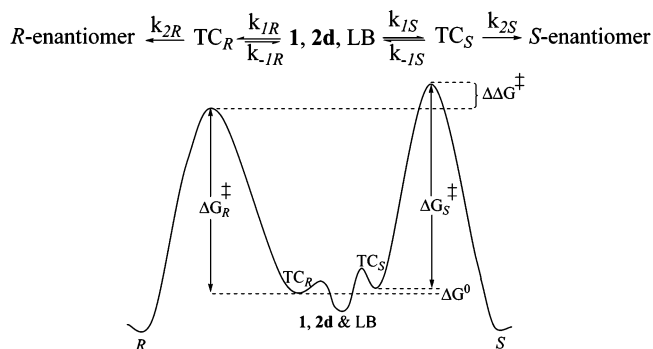


**FIGURE 5.** Energy diagram for origin of selectivity for electron-rich aldehydes.  $k_{2R}$  and  $k_{2S}$  are significantly small compared to  $k_{1R}$ ,  $k_{1S}$ ,  $k_{-1R}$ , and  $k_{-1S}$ , and they are determining factors for selectivity, which is strictly under Curtin-Hammett control.

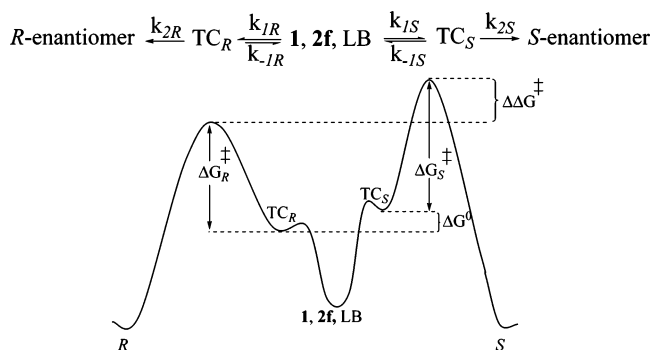


**FIGURE 6.** Energy diagram for origin of selectivity for electron-poor aldehydes.

be preserved and effectively transferred in the aldolization step. Intuitively, this stereochemical communication is most effective when the energy barrier for aldolization is small corresponding to an early aldolization transition state. The enhanced reactivity of the aldehyde carbonyl from its higher electrophilicity could account for a looser transition structure for aldolization, leading to larger value of  $A$  and less negative entropy of activation (Table 2).

Alternatively, the origin of selectivity observed for electron poor aldehydes can be understood in a different way. As discussed earlier, the attenuated Lewis basicity of the aldehyde carbonyl can lead to a higher energy barrier for the binding of the carbonyl oxygen to the silicon atom, or a smaller magnitude of  $k_{1R}$  and  $k_{1S}$  (Figure 6). At the same time, the enhanced reactivity of the aldehyde carbonyl accounts for greater  $k_{2R}$  and  $k_{2S}$ . In other words, increasing  $k_{1R}$  and  $k_{1S}$  goes in hand with decreasing  $k_{2R}$  and  $k_{2S}$ . In a limiting case, the magnitude of  $k_{1R}$  and  $k_{1S}$  becomes comparable to that of  $k_{2R}$  and  $k_{2S}$ . Consequently, the energy barrier for binding is now relatively large and contributes significantly to the overall energy barrier for the conversion of an unbound aldehyde into aldol enantiomers (Figure 6). The rate of formation of  $R$  and  $S$  aldol enantiomers depends both on  $k_{1R}$  and  $k_{2R}/k_{-1R}$  as well as  $k_{1S}$  and  $k_{2S}/k_{-1S}$ , respectively, which are reflected in the binding and aldolization steps.

According to this analysis, as the aldehyde carbonyl groups become more electron deficient (less Lewis basic), the greater the extent to which selectivity arising from



the binding event becomes important, and this accounts for a trend in selectivity observed in the right portion of the Hammett plot. Note that the selectivity garnered in binding is not complete unless rapid aldolization takes place. In other words, selectivity although originating from binding is still determined in aldolization.<sup>32</sup> This suggests that there should be no major change in the overall mechanism for the aldol reaction upon changing the electronic nature of aldehydes. This interpretation is consistent with the experimental results obtained from both the Arrhenius and the kinetic isotope effect studies.<sup>33</sup>

## Conclusion

The mechanism of the Lewis base-catalyzed enantioselective crossed-aldol reactions of aldehydes is proposed to involve three fundamental steps: ionization of chloride, binding of the aldehyde to the cationic silicon species, and aldolization. Of these, aldolization is the rate-determining step, as established through studies of <sup>12</sup>C/<sup>13</sup>C kinetic isotope effects at natural abundance. Arrhenius studies showed that the divergence of selectivity for electron-rich and electron poor aldehydes in the aldol reaction is not due to a change in the dominance of entropic or enthalpic contributions to the free energies of activation. Moreover, X-ray crystallographic studies ruled out the possibility that the aldol products are enantiomeric. Instead, the trends in selectivity for electron-rich and electron-poor aldehydes are interpreted according to the Hammond postulate and the Curtin–Hammett principle. The selectivity for electron-rich substrates is proposed to arise from the relatively late transition state for aldolization, and the aldol enantiomer distribution in this case is strictly under Curtin–Hammett control. As for electron-poor substrates, the selectivity presumably arises from a combination of the selective binding of the aldehyde to the siliconium atom and an early transition state for aldolization. Regardless of the electronic nature

(32) The ultimate stereochemical-determining event for both electron-rich and electron-poor aldehydes occurs in aldolization even though the origin of selectivity for each class of substrates comes from two different sources (binding and/or aldolization), which are influenced by the electronic natures of aldehydes. This also explains why there is a break in the Hammett plot.

(33) This mechanistic scenario falls under the boundary conditions for Curtin–Hammett principle: (a) Dauben, W. G.; Pitzer, K. S. In *Steric Effects in Organic Chemistry*; John Wiley & Sons: New York, 1956; Chapter 1. (b) Zefirov, N. S. *Tetrahedron* **1977**, *33*, 2719–2722. (c) Seeman, J. I.; Secor, H. V.; Hartung, H.; Galzerano, R. *J. Am. Chem. Soc.* **1980**, *102*, 7741–7747. (d) Seeman, J. I.; Sanders, E. B.; Farone, W. A. *Tetrahedron* **1980**, *36*, 1173–1177.

of aldehydes, there is no significant change in the overall mechanism for the aldol reaction.

## Experimental Section

**General Experimental Procedures.** See the Supporting Information.

**(R)-(2,2-Dimethoxy-1,1-dimethylethyl)benzenemethanol (4a).** To a stirred solution of **3** (84.3 mg, 0.1 mmol, 0.1 equiv) in 4 mL of chloroform/methylene chloride (4/1) at  $-78^{\circ}\text{C}$  was added enolate **1** (226.1 mg, 1.1 mmol, 1.1 equiv) dropwise via syringe. Five minutes later, freshly distilled benzaldehyde (102  $\mu\text{L}$ , 1.0 mmol) was added dropwise via syringe. The reaction mixture was stirred at  $-78^{\circ}\text{C}$  under  $\text{N}_2$  for 8 h. Dry methanol (15 mL) was then added dropwise at  $-78^{\circ}\text{C}$ , and the reaction mixture was stirred for 45 min. The solution was allowed to warm to room temperature (30 min) and was then quickly poured into a rapidly stirred, cold, aqueous sodium bicarbonate solution (25 mL). The resulting mixture was stirred at room temperature for 2 h. A cloudy white solution was observed during this period. The mixture was filtered through Celite, and the aqueous layer was separated and extracted with methylene chloride ( $3 \times 25\text{ mL}$ ). The combined organic layers were dried over sodium sulfate, filtered, and concentrated in vacuo. Silica gel column chromatography (hexanes/ethyl acetate, 5/1) followed by bulb-to-bulb distillation afforded 192.6 mg (86%) of **4a** as a clear, colorless oil: bp  $140^{\circ}\text{C}$  (0.02 mmHg, ABT); <sup>1</sup>H NMR (400 MHz,  $\text{CDCl}_3$ ) 7.23–7.33 (m, 5 H, H-aryl), 4.76 (d,  $J = 2.2$ , 1 H, HC(5)), 4.05 (s, 1 H, H(C(2))), 3.87 (d,  $J = 2.2$ , 1 H, OH), 3.58 (s, 3 H,  $\text{H}_3\text{C}$ (3)), 3.56 (s, 3 H,  $\text{H}_3\text{C}$ (3)), 0.92 (s, 3 H,  $\text{H}_3\text{C}$ (4)), 0.76 (s, 3 H,  $\text{H}_3\text{C}$ (4)); <sup>13</sup>C NMR (400 MHz,  $\text{CDCl}_3$ ) 141.13 (C(6)), 128.01 (C(7)), 127.47 (C(9)), 127.14 (C(8)), 114.02 (C(2)), 77.95 (C(5)), 58.82 (C(3)), 58.67 (C(3)), 43.62 (C(1)), 21.13 (C(4)), 17.04 (C(4)); IR ( $\text{CHCl}_3$ ) 3629 (w), 3479 (br), 3009 (s), 2942 (s), 2836 (m), 1471 (m), 1453 (m), 1390 (w), 1339 (w), 1237 (w), 1190 (m), 1104 (s), 1070 (s), 1016 (s), 955 (w), 705 (m); MS (FI) 224 ( $\text{M}^+$ , 0.4), 192 ( $\text{M}^+ - \text{MeOH}$ , 4), 106 ( $\text{C}_6\text{H}_5\text{CHO}$ , 33), 86 ( $(\text{CH}_3)_2\text{CCHOMe}$ , 100);  $[\alpha]_D^{24} -4.56$  ( $c = 0.74$ , EtOH); TLC  $R_f$  0.30 (hexane/EtOAc, 5/1) [silica gel, DNP]; SFC (*R*)-**4a**,  $t_R$  2.78 min (70.2%); (*S*)-**4a**,  $t_R$  3.19 min (29.8%) (column: OD, MeOH 5%, pressure 150 psi, flow 3.0 mL/min). Anal. Calcd for  $\text{C}_{13}\text{H}_{20}\text{O}_3$  (224.30) C, 69.61; H, 8.99. Found: C, 69.33; H, 9.02.

**Acknowledgment.** We are grateful to the National Science Foundation (NSF CHE-0105205 and CHE-0414440) for generous financial support. We thank Dr. G. L. Beutner for helpful discussions.

**Supporting Information Available:** General experimental procedures along with preparation and full characterization of aldol addition products. Procedures for kinetic runs of the aldol addition reaction, <sup>12</sup>C/<sup>13</sup>C kinetic isotope experiments, and all the kinetic data as well as average integrations for <sup>12</sup>C/<sup>13</sup>C KIE analysis. This material is available free of charge via the Internet at <http://pubs.acs.org>.

JO051680X